

Acta Cryst. (1994). **C50**, 981–984

Synthesis and Structures of Two Isostructural Phosphites, $\text{Fe}_{11}(\text{HPO}_3)_8(\text{OH})_6$ and $\text{Mn}_{11}(\text{HPO}_3)_8(\text{OH})_6$

MARTIN P. ATTFIELD, RUSSELL E. MORRIS
AND ANTHONY K. CHEETHAM

*Materials Department, University of California,
Santa Barbara, CA 93106, USA*

(Received 2 December 1993; accepted 1 February 1994)

Abstract

Iron hydroxyphosphite [undecairon octakis(hydrogenphosphite) hexahydroxide, $\text{Fe}_{11}(\text{HPO}_3)_8(\text{OH})_6$] and manganese hydroxyphosphite [undecamanganese octakis(hydrogenphosphite) hexahydroxide, $\text{Mn}_{11}(\text{HPO}_3)_8(\text{OH})_6$] were prepared hydrothermally in Teflon-lined steel autoclaves at 458 K. The compounds are isostructural with $\text{Zn}_{11}(\text{HPO}_3)_8(\text{OH})_6$. The structure contains highly distorted MO_6 octahedra, which share a common face to form M_2O_9 dimers. These dimeric units link together through two common edges to give infinite chains of dimers running along the [001] direction. Each chain is connected to four other such chains, by corner sharing, to form an open structure containing two types of channel, both of which run parallel to the *c* axis. One channel is triangular and occupied by one quarter of the phosphite groups, the other is hexagonal and lined by the remaining three quarters.

Comment

$\text{Fe}_{11}(\text{HPO}_3)_8(\text{OH})_6$ and $\text{Mn}_{11}(\text{HPO}_3)_8(\text{OH})_6$ are isostructural with $\text{Zn}_{11}(\text{HPO}_3)_8(\text{OH})_6$ (Marcos, Amoros & Le Bail, 1993). A projection of the structure along the [001] direction is shown in Fig. 1. The structures contain highly distorted MO_6 octahedra, made up of four O atoms from two phosphite groups [$\text{O}(2) \times 2$, $\text{O}(1)$ and $\text{O}(3)$] and two hydroxyl groups [$\text{O}(4) \times 2$]. The $\text{O}(4)$ atom is assumed to be the atom of the hydroxyl group by analogy with the Co, Ni and Zn compounds. The octahedra are highly distorted as pairs of octahedra share a common face [$\text{O}(3) - \text{O}(4) - \text{O}(4)$] to form M_2O_9 dimers. Such distortion is common in the condensation of octahedra and is seen here in the large deviations from 90° (up to 13.5 and 13° in the Fe and Mn derivatives, respectively) in the $\text{O} - \text{M} - \text{O}$ angles in the octahedra. These dimeric units link together through two common edges [$\text{O}(2) - \text{O}(4)$] to give infinite chains of dimers running along the [001] direction (see Fig. 2). Each chain is connected to four other such chains, by corner sharing, to form an open structure containing two types of channel, both of which run parallel to the *c*

axis. One channel is triangular and occupied by one quarter of the phosphite groups [P(2)] and the other is hexagonal and lined by the remaining three quarters of the phosphite groups [P(1)] (see Fig. 3). The hexagonal channels are lined by phosphite protons and are approximately 4 Å in diameter.

The two structures reported here extend the series of compounds with the general formula $\text{M}_{11}(\text{HPO}_3)_8(\text{OH})_6$, which contain partially occupied metal sites to maintain charge neutrality, as opposed to fully occupied metal sites and extra framework hydroxyl groups such as those in the structurally analogous compounds $\text{M}_3(\text{TeO}_3)_2(\text{OH})_2$ ($\text{M} = \text{Co}, \text{Ni}$). Both the Fe and Mn compounds are isostructural with $\text{Zn}_{11}(\text{HPO}_3)_8(\text{OH})_6$ and differ from the Ni and Co analogues only in respect of the orientation of the phosphite groups in the triangular channels.

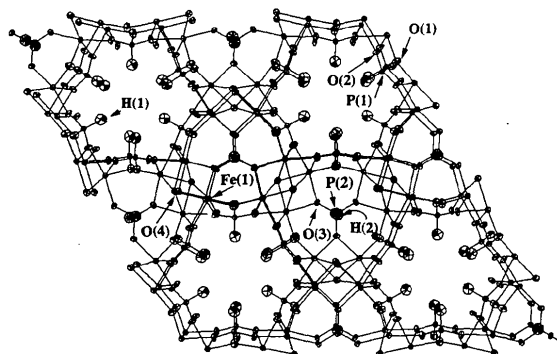


Fig. 1. The structure of $\text{Fe}_{11}(\text{HPO}_3)_8(\text{OH})_6$ viewed in the [001] direction showing the proton-lined channels. Displacement ellipsoids are shown at 50% probability. H atoms are shown as spheres of arbitrary size.

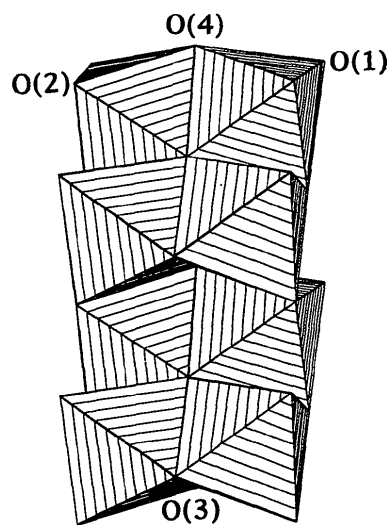


Fig. 2. Diagram of one of the chains of dimers formed by edge sharing of the $[\text{Fe}_2\text{O}_9]$ dimeric units.

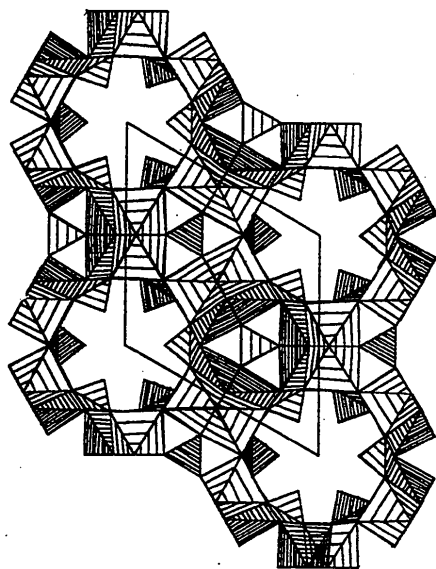


Fig. 3. Polyhedral representation of the structure of Fe₁₁(HPO₃)₈(OH)₆ viewed along the [001] direction. The differently hatched [FeO₆] octahedra and [HPO₃] pseudo-tetrahedra are at different *z* levels (*z* and *z* + $\frac{1}{2}$).

Experimental

Fe₁₁(HPO₃)₈(OH)₆ was prepared in a 23 ml capacity Teflon-lined steel autoclave from a reaction mixture (pH *ca* 7) containing FeCl₃·6H₂O (1.32 g), H₃PO₃ (0.6 g) and NaOH (0.894 g) in 17 ml of deionized water. The reaction mixture was heated for 100 h at 485 K and then cooled at 10 K min⁻¹ to room temperature. Colorless needle-like crystals, embedded in a black amorphous material, were recovered from the reaction mixture.

Mn₁₁(HPO₃)₈(OH)₆ was prepared following the same procedure used for the iron derivative, but using a reaction mixture (pH *ca* 7) containing MnCl₂·4H₂O (1.9 g), H₃PO₃ (0.5 g) and NaOH (0.7077 g). The product was recovered as a pink microcrystalline powder.

Fe₁₁(HPO₃)₈(OH)₆

Crystal data

M_r = 1356.1

Hexagonal

*P*6₃*mc*

a = 12.9994 (8) Å

c = 5.0932 (3) Å

V = 745.36 (8) Å³

Z = 1

Cu *K*α radiation

λ = 1.5418 Å

Cell parameters from 25 reflections

θ = 18.957–27.829°

μ = 47.1 mm⁻¹

T = 293 K

Needle

0.3 × 0.03 × 0.01 mm

Colorless

Data collection

Enraf-Nonius CAD-4-MACH diffractometer

ω-2θ scans

Absorption correction:

DIFABS (Walker & Stuart, 1983)

*T*_{min} = 0.53, *T*_{max} = 0.75

289 observed reflections

[*I* > 3σ(*I*)]

*R*_{int} = 0.0267

θ_{max} = 36°

h = -1 → 16

k = -16 → 16

l = -1 → 6

2089 measured reflections
361 independent reflections

3 standard reflections
frequency: 60 min
intensity variation: none

Refinement

Refinement on *F*

R = 0.0243

wR = 0.0283

289 reflections

47 parameters

H-atom parameters not refined

Calculated weights based on Tukey-Prince algorithm (using Chebyshev polynomial)

(Δ/σ)_{max} = 0.01

Δρ_{max} = 1.34 e Å⁻³

Δρ_{min} = -0.613 e Å⁻³

Atomic scattering factors from *International Tables for X-ray Crystallography* (1974, Vol. IV)

Table 1. Fractional atomic coordinates, equivalent isotropic displacement parameters (Å²) and site occupancy factors for Fe₁₁(HPO₃)₈(OH)₆

*U*_{eq} = (*U*₁*U*₂*U*₃)^{1/3}, where *U*_{*i*} are the principle axes of the displacement ellipsoid.

	<i>x</i>	<i>y</i>	<i>z</i>	<i>U</i> _{eq}	Atom site occupancy
Fe(1)	0.57219 (7)	0.65171 (7)	0.0610 (5)	0.0139	0.916 (7)
P(1)	0.84022 (8)	1 - <i>x</i>	0.0439 (7)	0.0135	1.0
P(2)	1/3	2/3	0.8309 (8)	0.0127	1.0
O(1)	0.8042 (3)	1 - <i>x</i>	0.792 (1)	0.0216	1.0
O(2)	0.6588 (4)	0.9259 (4)	0.7047 (8)	0.0185	1.0
O(3)	0.6025 (2)	1 - <i>x</i>	0.415 (2)	0.0203	1.0
O(4)	0.5249 (2)	1 - <i>x</i>	0.870 (1)	0.0186	1.0

Table 2. Selected geometric parameters (Å, °) for Fe₁₁(HPO₃)₈(OH)₆

Fe(1)—O(1 ⁱ)	2.146 (5)	P(1)—O(2 ^{vi})	1.518 (5)
Fe(1)—O(2 ⁱⁱ)	2.171 (4)	P(1)—O(2 ^{vii})	1.518 (5)
Fe(1)—O(2 ⁱⁱⁱ)	2.118 (5)	P(1)—H(1 ^v)	1.298
Fe(1)—O(3 ^{iv})	2.161 (5)	P(2)—O(3 ^{viii})	1.506 (3)
Fe(1)—O(4 ^v)	2.277 (4)	P(2)—O(3 ^{ix})	1.506 (6)
Fe(1)—O(4 ^{iv})	2.169 (5)	P(2)—O(3 ^x)	1.506 (3)
P(1)—O(1 ^v)	1.516 (7)	P(2)—H(2)	1.298
O(2 ⁱⁱ)—Fe(1)—O(1 ⁱ)	90.8 (1)	O(4 ^{iv})—Fe(1)—O(4 ^v)	77.5 (1)
O(2 ⁱⁱⁱ)—Fe(1)—O(1 ⁱ)	101.2 (2)	O(2 ^{vi})—P(1)—O(1 ^v)	111.7 (2)
O(3 ^{iv})—Fe(1)—O(1 ⁱ)	100.1 (2)	O(2 ^{vii})—P(1)—O(1 ^v)	111.7 (2)
O(4 ^v)—Fe(1)—O(1 ⁱ)	171.9 (2)	H(1 ^v)—P(1)—O(1 ^v)	107.0
O(4 ^{iv})—Fe(1)—O(1 ⁱ)	94.6 (2)	O(2 ^{vii})—P(1)—O(2 ^{vi})	111.5 (4)
O(2 ⁱⁱⁱ)—Fe(1)—O(2 ⁱⁱ)	90.4 (2)	H(1 ^v)—P(1)—O(2 ^{vi})	107.3
O(3 ^{iv})—Fe(1)—O(2 ⁱⁱ)	167.2 (2)	H(1 ^v)—P(1)—O(2 ^{vii})	107.3
O(4 ^v)—Fe(1)—O(2 ⁱⁱ)	87.5 (2)	O(3 ^{ix})—P(2)—O(3 ^{viii})	112.3 (4)
O(4 ^{iv})—Fe(1)—O(2 ⁱⁱ)	88.3 (2)	O(3 ^x)—P(2)—O(3 ^{viii})	112.3 (4)
O(3 ^{iv})—Fe(1)—O(2 ⁱⁱⁱ)	94.0 (2)	H(2)—P(2)—O(3 ^{viii})	106.5
O(4 ^v)—Fe(1)—O(2 ⁱⁱⁱ)	86.8 (2)	O(3 ^x)—P(2)—O(3 ^{ix})	112.3 (4)
O(4 ^{iv})—Fe(1)—O(2 ⁱⁱⁱ)	164.2 (2)	H(2)—P(2)—O(3 ^{ix})	106.5
O(4 ^v)—Fe(1)—O(3 ^{iv})	80.8 (2)	H(2)—P(2)—O(3 ^x)	106.5
O(4 ^{iv})—Fe(1)—O(3 ^{iv})	84.2 (2)		

Symmetry codes: (i) *x* - *y*, *x*, *z* - $\frac{1}{2}$; (ii) 1 + *x* - *y*, *x*, *z* - $\frac{1}{2}$; (iii) *x*, 1 + *x* - *y*, *z* - 1; (iv) 1 - *x*, 1 - *y*, *z* - $\frac{1}{2}$; (v) *x*, *y*, *z* - 1; (vi) *y*, -*x* + *y*, *z* - $\frac{1}{2}$; (vii) 1 + *x* - *y*, 1 - *y*, *z* - $\frac{1}{2}$; (viii) *x* - *y*, *x*, $\frac{1}{2}$ + *z*; (ix) 1 - *x*, 1 - *y*, $\frac{1}{2}$ + *z*; (x) *y*, 1 - *x* + *y*, $\frac{1}{2}$ + *z*.

Mn₁₁(HPO₃)₈(OH)₆*Crystal data* $M_r = 1346.2$

Hexagonal

 $P6_3mc$ $a = 13.1957 (6) \text{ \AA}$ $c = 5.1770 (3) \text{ \AA}$ $V = 780.68 (8) \text{ \AA}^3$ $Z = 1$ Cu $K\alpha$ radiation $\lambda = 1.54178 \text{ \AA}$ *Data collection*

High-resolution Scintag

PAD-X diffractometer

 θ - θ scans $\theta_{\max} = 57.5^\circ$ *Refinement* $R_{wp} = 0.2024$ $R_p = 0.1453$ $R_F = 0.0768$

30 least-squares parameters

Atomic scattering factors

from *International Tables*for *X-ray Crystallography*

(1974, Vol. IV)

Table 3. Fractional atomic coordinates, isotropic displacement parameters (\AA^2) and site occupancy factors for Mn₁₁(HPO₃)₈(OH)₆

	<i>x</i>	<i>y</i>	<i>z</i>	U_{iso}	Atom site occupancy
Mn(1)	0.5730 (3)	0.6529 (3)	0.0700	0.0098 (7)	0.915 (8)
P(1)	0.8391 (3)	1 - <i>x</i>	0.050 (3)	0.0094 (7)	1.0
P(2)	1/3	2/3	0.826 (3)	0.0086 (7)	1.0
O(1)	0.8050 (7)	1 - <i>x</i>	0.809 (4)	0.0175 (7)	1.0
O(2)	0.654 (1)	0.9200 (9)	0.714 (2)	0.0144 (7)	1.0
O(3)	0.6043 (7)	1 - <i>x</i>	0.425 (3)	0.0162 (7)	1.0
O(4)	0.5255 (8)	1 - <i>x</i>	0.891 (3)	0.0145 (7)	1.0

Table 4. Selected geometric parameters (\AA , $^\circ$) forMn₁₁(HPO₃)₈(OH)₆

Mn(1)—Mn(1 ⁱ)	2.981 (7)	P(1)—O(2 ^{vii})	1.52 (1)
Mn(1)—O(1 ⁱⁱ)	2.19 (1)	P(1)—O(2 ^{viii})	1.52 (1)
Mn(1)—O(2 ⁱⁱⁱ)	2.25 (1)	P(1)—H(1 ^{vi})	1.30
Mn(1)—O(2 ^{iv})	2.133 (9)	P(2)—O(3 ^{ix})	1.52 (2)
Mn(1)—O(3 ^v)	2.22 (1)	P(2)—O(3 ^x)	1.52 (2)
Mn(1)—O(4 ^{vi})	2.31 (2)	P(2)—O(3 ^{xi})	1.52 (2)
Mn(1)—O(4 ^v)	2.26 (1)	P(2)—H(2)	1.29
P(1)—O(1 ^{vi})	1.47 (2)		
O(2 ⁱⁱⁱ)—Mn(1)—O(1 ⁱⁱ)	91.7 (5)	O(4 ^v)—Mn(1)—O(4 ^{vi})	76.9 (4)
O(2 ^{iv})—Mn(1)—O(1 ⁱⁱ)	101.6 (5)	O(2 ^{vii})—P(1)—O(1 ^{vi})	112.1 (7)
O(3 ^v)—Mn(1)—O(1 ⁱⁱ)	100.1 (5)	O(2 ^{viii})—P(1)—O(1 ^{vi})	112.1 (7)
O(4 ^{vi})—Mn(1)—O(1 ⁱⁱ)	169.4 (5)	H(1 ^{vi})—P(1)—O(1 ^{vi})	103.3
O(4 ^v)—Mn(1)—O(1 ⁱⁱ)	92.8 (5)	O(2 ^{vii})—P(1)—O(2 ^{vii})	108.1 (11)
O(2 ^{iv})—Mn(1)—O(2 ⁱⁱⁱ)	92.7 (4)	H(1 ^{vi})—P(1)—O(2 ^{vii})	110.5
O(3 ^v)—Mn(1)—O(2 ⁱⁱⁱ)	165.8 (4)	H(1 ^{vi})—P(1)—O(2 ^{viii})	110.5
O(4 ^{vi})—Mn(1)—O(2 ⁱⁱⁱ)	85.0 (4)	O(3 ^x)—P(2)—O(3 ^{ix})	109.1 (9)
O(4 ^v)—Mn(1)—O(2 ⁱⁱⁱ)	87.2 (5)	O(3 ^{xi})—P(2)—O(3 ^{ix})	109.1 (9)
O(3 ^v)—Mn(1)—O(2 ^{iv})	92.6 (5)	H(2)—P(2)—O(3 ^{ix})	109.8
O(4 ^{vi})—Mn(1)—O(2 ^{iv})	88.6 (5)	O(3 ^{xi})—P(2)—O(3 ^x)	109.1 (8)
O(4 ^v)—Mn(1)—O(2 ^{iv})	165.5 (5)	H(2)—P(2)—O(3 ^x)	109.8
O(4 ^{vi})—Mn(1)—O(3 ^v)	81.9 (6)	H(2)—P(2)—O(3 ^{xi})	109.8
O(4 ^v)—Mn(1)—O(3 ^v)	84.4 (5)		

Symmetry codes: (i) 1 - *y*, 1 - *x*, *z*; (ii) *x* - *y*, *x*, *z* - $\frac{1}{2}$; (iii) 1 + *x* - *y*, *x*, *z* - $\frac{1}{2}$; (iv) *x*, 1 + *x* - *y*, *z* - 1; (v) 1 - *x*, 1 - *y*, *z* - $\frac{1}{2}$; (vi) *x*, *y*, *z* - 1; (vii) *y*, -*x* + *y*, *z* - $\frac{1}{2}$; (viii) 1 + *x* - *y*, 1 - *y*, *z* - $\frac{1}{2}$; (ix) *x* - *y*, *x*, $\frac{1}{2}$ + *z*; (x) 1 - *x*, 1 - *y*, $\frac{1}{2}$ + *z*; (xi) *y*, 1 - *x* + *y*, $\frac{1}{2}$ + *z*.

Room-temperature X-ray intensity data were collected on a single crystal of Fe₁₁(HPO₃)₈(OH)₆. Data collection was performed using Enraf-Nonius diffractometer software. Data reduction was performed using RC85 (Baird, 1987). The systematic absences were consistent with those of the space groups $P6_3mc$, $P6_2c$ and $P6_3/mmc$. $P6_3mc$ was chosen, as this was the

space group of the framework structure of Ni₃(TeO₃)₂(OH)₂ (Perez, Lasserre, Moret & Maurin, 1976), which was used as the starting model for the refinement. *CRYSTALS* (Watkin, Caruthers & Betteridge, 1989) was used to refine the structure. No indication of the presence of any extra framework atoms was found in the difference Fourier maps, so the site occupancy factor of the Fe atom was refined to compensate for the charge imbalance. No evidence for the inversion of any of the HPO₃ pseudo-tetrahedra on the threefold axis was found in the difference Fourier maps, unlike the cases of $M_{11}(\text{HPO}_3)_8(\text{OH})_6$ ($M = \text{Co}, \text{Ni}$) (Marcos, Amoros, Beltran-Porter, Martinez-Manez & Attfield, 1993). Refinement of the Flack enantiomorph parameter (Flack, 1983) gave a value close to 1, so the structure was inverted. The phosphite H atoms were placed in chemically reasonable positions using distances and angles with standard values for phosphite groups in this type of compound. The final cycle of least-squares refinement included the positional and anisotropic displacement parameters for Fe, P and O, and the site-occupancy factor of Fe. As the $P6_3mc$ space group is polar, the origin was fixed at the centroid of the structure. The H-atom positions and displacement parameters were left unrefined.

The X-ray powder diffraction data initially collected for Mn₁₁(HPO₃)₈(OH)₆ indicated that this phase was isostructural with Fe₁₁(HPO₃)₈(OH)₆. High-resolution powder X-ray data were collected on a Scintag PAD-X diffractometer operating in θ - θ geometry ($\lambda = 1.54178 \text{ \AA}$) between $2\theta = 5$ and 115° , using a step size of 0.02° . Rietveld profile analysis was performed on 4848 data points between $2\theta = 18$ and 115° , thus excluding two largely asymmetric low-angle peaks. The analysis was performed using the program GSAS (Larson & Von Dreele, 1987), using the starting model obtained from the structure solution of Fe₁₁(HPO₃)₈(OH)₆. The *z* coordinate of the Mn atom was fixed in the refinement as the space group $P6_3mc$ is polar and the isotropic displacement parameters of the non-H atoms were constrained to have the same shift. The final cycle of least-squares refinement included the scale factor, detector zero-point correction, background coefficients, unit-cell parameters, and peak shape-width variation terms (pseudo-Voigt), in addition to the positional and isotropic displacement parameters of Mn, P and O, and the fractional occupancy of Mn. The H-atom positions and displacement parameters were left unrefined. Final observed, calculated and difference profile plots are shown in Fig. 4. Attempts to improve the fit by inverting a fraction of the

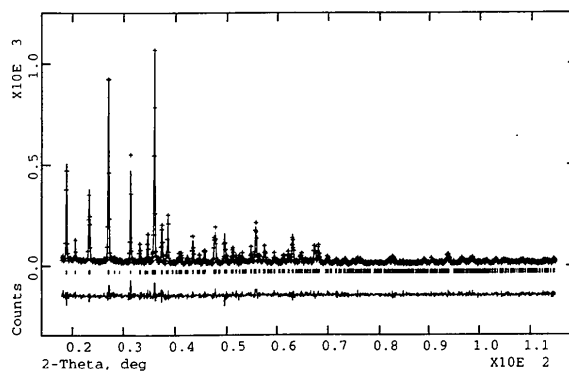


Fig. 4. Final observed (crosses), calculated (line), reflection markers (ticks) and difference profile plots for Mn₁₁(HPO₃)₈(OH)₆.

phosphite groups on the threefold axis gave either unstable refinements or chemically unreasonable structures, hence all were left in the same orientation as in the Fe compound.

MPA would like to acknowledge the University of California, Santa Barbara, for the provision of a scholarship.

Lists of structure factors, anisotropic displacement parameters, H-atom coordinates and complete geometry for Fe₁₁(HPO₃)₈(OH)₆, and primary powder diffraction data and H-atom coordinates for Mn₁₁(HPO₃)₈(OH)₆ have been deposited with the IUCr (Reference: BR1071). Copies may be obtained through The Managing Editor, International Union of Crystallography, 5 Abbey Square, Chester CH1 2HU, England.

References

- Baird, P. D. (1987). *RC85*. Chemical Crystallography Laboratory, Univ. of Oxford, England.
- Flack, H. (1983). *Acta Cryst.* **A39**, 876–881.
- Larson, A. C. & Von Dreele, R. B. (1987). Report No. LA-UR-86-748. Los Alamos Laboratory, USA.
- Marcos, M. D., Amoros, P., Beltran-Porter, A., Martinez-Manez, R. & Attfield, J. P. (1993). *Chem. Mater.* **5**, 121–128.
- Marcos, M. D., Amoros, P. & Le Bail, A. (1993). *J. Solid State Chem.* **107**, 250–257.
- Perez, G., Lasserre, F., Moret, J. & Maurin, M. (1976). *J. Solid State Chem.* **17**, 143–149.
- Walker, N. & Stuart, D. (1983). *A39*, 158–166.
- Watkin, D. J., Carruthers, J. R. & Betteridge, P. W. (1989). *CRYSTALS User Guide*. Chemical Crystallography Laboratory, Univ. of Oxford, England.

Acta Cryst. (1994). **C50**, 984–986

Rietveld Refinement of Dry-Synthesized Rb₂ZnSi₅O₁₂ Leucite by Synchrotron X-ray Powder Diffraction

A. M. T. BELL

SERC Daresbury Laboratory, Daresbury, Warrington, Cheshire WA4 4AD, England

C. M. B. HENDERSON

Department of Geology, University of Manchester, Manchester M13 9PL, England

(Received 6 December 1993; accepted 15 February 1994)

Abstract

Analysis of a high-resolution synchrotron X-ray powder diffraction pattern of a dry-synthesized rubidium zinc silicate, leucite analogue Rb₂ZnSi₅O₁₂, showed that this material has a cubic *la3d* structure. The structure of this material has been refined by the Rietveld method. Si and Zn

atoms are disordered on tetrahedral framework sites and Rb occupies large channel sites along the [111] direction.

Comment

As part of a wider attempt to understand the controls and consequences of tetrahedral-cation ordering, we are studying a series of synthetic leucite analogues X₂Z^{II}Si₅O₁₂ (X = K, Rb, Cs; Z = Mg, Zn, Cd) in silicates with framework structures related to natural leucite (KAlSi₂O₆) by the coupled framework cation substitution 2Al = Z, Si (Torres-Martinez & West, 1989). Such compounds are more amenable to tetrahedral site (*T*-site) analysis than Al/Si analogues and also display significantly different *T*-site ordering arrangements depending on their conditions of synthesis and chemical compositions.

X-ray powder diffraction techniques and Rietveld analysis (Rietveld, 1969) were used to determine the crystal structures of these materials, together with ²⁹Si magic-angle spinning NMR spectroscopy, to characterize the number of distinct Si sites. Some of the leucite analogues we have studied have known leucite-type structures, but we have also determined previously unknown monoclinic (*P2₁/c*; Bell, Henderson, Redfern, Cernik, Champness, Fitch & Kohn, 1994) and orthorhombic (*Pbca*; Bell, Redfern, Henderson & Kohn, 1994) structures which have the basic leucite topology. In this paper we describe the structure of a dry-synthesized leucite with the stoichiometry Rb₂ZnSi₅O₁₂.

Analysis of the powder diffraction data showed (from the systematic absences) that this material has a cubic *la3d* structure. Therefore, atomic coordinates for the *la3d* structure of dry-synthesized K₂MgSi₅O₁₂ (Bell, Henderson, Redfern, Cernik, Champness, Fitch & Kohn, 1994) were used as a starting model for Rietveld refinement. The Rb₂ZnSi₅O₁₂ structure was then refined using the *MPROF* program of the *Powder Diffraction Program Library (PDPL)* (Murray, Cockcroft & Fitch, 1990). The observed and calculated profiles in the Rietveld difference plot were a good match (Fig. 1) indicating that the refined structure is reliable.

The *la3d* structure is characterized by having a single *T* site and the tetrahedral cations must be disordered on this site. Thus the leucite-group natural mineral, pollucite (CsAlSi₂O₆; Beger, 1969), has disordered Si and Al arrangements, while dry-synthesized Rb₂ZnSi₅O₁₂ has disordered Si and Zn. Other synthetic leucites are also cubic *la3d* (Bell, Henderson, Redfern, Cernik, Champness, Fitch & Kohn, 1994; Torres-Martinez & West, 1989) with similarly disordered tetrahedral cations.

The refined *T*—O distances of the title compound represent the weighted average of tetrahedrally coordinated Si—O and Zn—O bond lengths of the disordered framework. The distortions in the framework structure resulting from the presence of Zn in *T* sites are also reflected in the range of O—*T*—O angles of 103–113° [cf. 102–119° in dry-synthesized Rb₂MgSi₅O₁₂ (Torres-Martinez